NASA
Technical
Paper
2873

November 1988

Control Surface Spanwise Placement in Active Flutter Suppression Systems

E. Nissim and
John J. Burken

NASA

ıSA
chnical
per
73

ı8

Control Surface Spanwise Placement in Active Flutter Suppression Systems

E. Nissim and
John J. Burken
Ames Research Center
Dryden Flight Research Facility
Edwards, California

National Aeronautics
and Space Administration

**Scientific and Technical
Information Division**

SUMMARY

A method is developed that determines the placement of an active control surface for maximum effectiveness in suppressing flutter. No specific control law is required by this method which is based on the aerodynamic energy concept. It is argued that the spanwise placement of the active controls should coincide with the locations where maximum energy per unit span is fed into the system. The method enables one to determine the distribution, over the different surfaces of the aircraft, of the energy input into the system as a result of the unstable fluttering mode. The method is illustrated using three numerical examples.

INTRODUCTION

All active flutter suppression systems require sensors to detect the movement of the lifting surface and to activate a control surface according to a synthesized control law. Most of the work performed to date (Mahesh and others, 1981; Mukhopadhyay and others, 1981; Newsom, 1979; Nissim and Abel, 1978; Nissim and others, 1976) relate to the development of control laws based on predetermined locations of sensors and control surfaces.These locations of sensors and control surfaces are determined either arbitrarily, or by means of a trial and error procedure (Nissim and others, 1976).

The aerodynamic energy approach developed in Nissim (1971) indicates that the sensors should be on the same streamwise strip where the activated control surface is placed, much in accord with Wykes' identically located accelerometer force (ILAF) concept (Wykes and Mori, 1965). The aerodynamic energy concept also indicates (Nissim, 1977, p. 25) that the best chordwise location of a sensor activating a trailing edge control surface is around the 65-percent chord location. The best chordwise location for a sensor activating a leading edge surface is shown to lie upstream of the wing (20-percent chord upstream of the leading edge), or alternatively, two sensors located along the same chord should be used.

Recent work relating to mass-unbalance effects of control surfaces indicates that the spanwise location of the sensors within the control surface strip is related to the spanwise location of the center of gravity of the control surface and to the centroid of the strip's surface. The determination of the best spanwise placement of an active control surface for flutter suppression using a methodical approach rather than by trial and error is the primary topic of this paper.

The authors describe a method that determines the aforementioned spanwise placement of the activated control surface without resorting to any specific control law. The method is based on the aerodynamic energy concept whereby the activated control surface is placed at the location where most of the energy is fed into the unstable structure. The following analysis will assume, for sake of simplicity, that the generalized aerodynamic forces are obtained using a doublet-lattice program. This is done for purposes of illustration only, and the method can be applied to any form of calculation of the generalized aerodynamic forces.

NOMENCLATURE

a_i	area of box i
b	semichord length
$h_{ij_{3/4}}$	deflection at 3/4-chord point of box i due to deflection of mode j

$\bar{h}_{ij_{3/4}}$	$h_{ij_{3/4}}/b$
$h_{ij_{1/4}}$	deflection of $1/4$-chord point of box i due to deflection of mode j
k	reduced frequency $(\omega b/V)$
ℓ	number of strips on the lifting surfaces
m	number of boxes
n	number of modes
Q	dynamic pressure
Q_F	flutter dynamic pressure
q_i	ith generalized coordinate
s_r	span of boxes at the rth strip
V	flight velocity
W	work
W_A	total work done by system per cycle of oscillation
W_A^r	work done by strip r per cycle of oscillation
$\bar{W}_A^r$	W_A^r/W_A
$\bar{\bar{W}}_A^r$	$\bar{W}_A^r/s_r$
$\alpha_{ij_{3/4}}$	slope at $3/4$-chord point of box i due to deflection of mode j
ω	frequency of oscillation
ω_F	flutter frequency

Matrices

$\lfloor\ \rfloor$	row matrix
$\{\ \}$	column matrix
$\lceil\ \rfloor$	diagonal matrix
$*$	conjugate
$[A]$	$[A_R] + i[A_I]$
$[A]^r$	aerodynamic matrix due to rth strip
$[A_I]$	imaginary part of aerodynamic matrix
$[A_R]$	real part of aerodynamic matrix
$[C]$	matrix relating boxes to specific strip, defined in equation (15)
$\{F\}$	force vector with element i denoting the force acting on box i
$[H]_{1/4}$	matrix the elements of which are h_{ij} at the quarter chord location
$[H]_{3/4}$	matrix defined by equation (3)
$\{p\}$	vector denoting unsteady aerodynamic pressures at the different boxes
$[P]$	matrix defined by equation (6)
$[\bar{P}]$	influence coefficient matrix relating downwash to pressures (see equation (4))
$\{Q\}$	vector denoting generalized aerodynamic forces
$\{q_o\}$	vector denoting the generalized complex eigenvector associated with the fluttering mode
$\left\{\frac{w}{V}\right\}_{3/4}$	vector denoting the downwash slopes at the 3/4-chord point of the various boxes
$\{z\}_{1/4}$	vector denoting deflections at the 1/4-chord point of the various boxes

GENERAL APPROACH

The Strip Contribution to the Aerodynamic Matrix

Assume the lifting surfaces are divided into boxes that form a number of strips along their spans. The doublet lattice method (Albano and Rodden, 1969) determines the pressure in each box as a function of the downwash velocities $\{W\}_{3/4}$ at the $3/4$-chord locations of the different boxes, where

$$\{W\}_{3/4} = V \begin{bmatrix} \alpha_{11} & \alpha_{12} & \cdots & \alpha_{1n} \\ \alpha_{21} & \alpha_{22} & \cdots & \alpha_{2n} \\ \vdots & & & \\ \alpha_{m1} & \alpha_{m2} & \cdots & \alpha_{mn} \end{bmatrix}_{3/4} \begin{Bmatrix} q_1 \\ q_2 \\ \vdots \\ q_n \end{Bmatrix} + i\omega \begin{bmatrix} h_{11} & h_{12} & \cdots & h_{1n} \\ h_{21} & h_{22} & \cdots & h_{2n} \\ \vdots & & & \\ h_{m15} & h_{m2} & \cdots & h_{mn} \end{bmatrix}_{3/4} \begin{Bmatrix} q_1 \\ q_2 \\ \vdots \\ q_n \end{Bmatrix} \tag{1}$$

where n denotes the number of modes, m denotes the number of boxes, and α_{ij} is the slope of the $3/4$-chord point of box i as a result of the deformation described by mode j. Similarly, h_{ij} describes the deflection at the $3/4$-chord point of box i due to mode j and q_i denotes the ith generalized coordinate. The parameters V and ω describe, respectively, the fluid velocity and the frequency of oscillation. The deformation h_{ij} can be nondimensionalized using a reference semichord length b, that is,

$$\bar{h}_{ij_{3/4}} = \frac{h_{ij_{3/4}}}{b} \tag{2}$$

Therefore, equation (1) assumes the form

$$\left\{\frac{W}{V}\right\}_{3/4} = [H]_{3/4}\{q\} \tag{3}$$

where

$$[H]_{3/4} = \begin{bmatrix} \alpha_{11} & \alpha_{12} & \cdots & \alpha_{1n} \\ \alpha_{21} & \alpha_{22} & \cdots & \alpha_{2n} \\ \vdots & & & \\ \alpha_{m1} & \alpha_{m2} & \cdots & \alpha_{mn} \end{bmatrix}_{3/4} + ik \begin{bmatrix} \bar{h}_{11} & \bar{h}_{12} & \cdots & \bar{h}_{1n} \\ \bar{h}_{21} & \bar{h}_{22} \cdots & \bar{h}_{2n} & \\ \vdots & & & \\ \bar{h}_{m1} & \bar{h}_{m2} & \cdots & \bar{h}_{mn} \end{bmatrix}_{3/4}$$

and

$$k = \frac{\omega b}{V}$$

$$\{q\} = \begin{Bmatrix} q_1 \\ q_2 \\ \vdots \\ q_n \end{Bmatrix}$$

The doublet lattice method yields the pressures in each of the boxes in the form

$$\{p\} = [\bar{P}] \left\{ \frac{W}{V} \right\}_{3/4} \tag{4}$$

Substituting equation (3) into equation (4) one obtains

$$\{p\} = [P]\{q\} \tag{5}$$

where

$$[P] = [\bar{P}][H]_{3/4} \tag{6}$$

Let the vector $\{z\}_{1/4}$ describe the deflections at the $1/4$-chord point of each box. The $\{z\}_{1/4}$ vector can be written in the form

$$\{z\}_{1/4} = [H]_{1/4}\{q\} \tag{7}$$

where

$$[H]_{1/4} = \begin{bmatrix} h_{11} & h_{12} & \cdots & h_{1n} \\ h_{21} & h_{22} & \cdots & h_{2n} \\ \vdots & & & \\ h_{m1} & h_{m2} & \cdots & h_{mn} \end{bmatrix}_{1/4} \tag{8}$$

represents the modal deflections at the $1/4$-chord point of the different boxes. The total force acting on each box is therefore given by

$$\{F\} = \begin{bmatrix} a_1 & & & \\ & a_2 & & \\ & & \ddots & \\ & & & a_m \end{bmatrix} [P]\{q\} \tag{9}$$

where a_i denotes the area of box i. The virtual work $\delta(W)$ done by these forces is given by

$$\delta(W) = \lfloor \delta q \rfloor [H^T]_{1/4}\{F\}$$

so that the generalized forces are given by

$$\{Q\} = [H^T]_{1/4}\{F\} \tag{10}$$

where $[H^T]$ denotes the transpose of matrix [H].

Using equation (9), equation (10) can be written as

$$\{Q\} = [A]\{q\} \tag{11}$$

where

$$[A] = [H^T]_{1/4} \lceil a \rfloor [P] \tag{12}$$

Equation (12) indicates that the element A_{ij} is given by

$$A_{ij} = \sum_{k=1}^{m} h_{ki_{1/4}} a_k P_{kj} \tag{13}$$

At this point it is important to note that the summation in equation (13) reflects the contribution to the virtual work of all the forces acting on each of the m boxes. Let us consider the contribution to the generalized forces of the boxes on the rth strip and denote this contribution by A_{ij}^r, where

$$A_{ij}^r = \sum_{k=1}^{m} h_{ki_{1/4}} a_k P_{kj} C_{kr} \tag{14}$$

where $C_{kr} = 0$ for all boxes which do not lie on the rth strip and $C_{kr} = 1$ for all boxes lying on the rth strip. C can be arranged in the matrix form

$$[C] = [\{C_{k1}\}\{C_{k2}\}\cdots\{C_{k\ell}\}] \tag{15}$$

where $[C]$ is of order $m \times \ell$, with ℓ denoting the number of strips on the lifting surfaces.

Clearly, A_{ij} is obtained by summing up the contributions of all the strips, that is,

$$A_{ij} = \sum_{r=1}^{\ell} A_{ij}^r \tag{16}$$

Based on equations (14) and (15), ℓ aerodynamic matrices $[A]^r$ can be obtained, one for each strip, representing the contribution of each strip to the generalized aerodynamic matrix $[A]$. Clearly,

$$[A] = \sum_{r=1}^{\ell} [A]^r \tag{17}$$

The Work Done by the Aerodynamic Forces

It is shown in Nissim (1971) that the work W_A done by the system on its surroundings per one cycle of oscillation is given by

$$W_A = \frac{\pi}{2} \lfloor q_o^* \rfloor \left(- \left[A_I + A_I^T \right] + i \left[A_R - A_R^T \right] \right) \{q_o\} \tag{18}$$

where $\{q_o\}$ is the complex eigenvector of the fluttering mode and $\{q_o^*\}$ denotes its complex conjugate. The real matrices $[A_R]$ and $[A_I]$ are derived from $[A]$ following the definition

$$[A] = [A_R] + i[A_I] \tag{19}$$

Following the derivation in the previous section of this work of the strips' aerodynamic matrices, the work W_A^r done by the rth strip on its surroundings per one cycle of oscillation can be written in a form which is identical to equation (18), that is,

$$W_A^r = \frac{\pi}{2} \lfloor q_o^* \rfloor \left(- \left[A_I + A_I^T \right]^r + i \left[A_R - A_R^T \right]^r \right) \{q_o\} \tag{20}$$

where $[A_r]^r$ and $[A_i]^r$ are real matrices defined by

$$[A]^r = [A_R]^r + i[A_I]^r \tag{21}$$

At this stage the energy ratio $\bar{W}_A^r$ of the rth strip will be defined by

$$\bar{W}_A^r = \frac{W_A^r}{|W_A|} \tag{22}$$

and the specific energy ratio $\bar{\bar{W}}_A^r$ of the rth strip will be defined by

$$\bar{\bar{W}}_A^r = \frac{\bar{W}_A^r}{s_r} \tag{23}$$

where s_r denotes the span of the rth strip.

It should be noted that the specific energy ratio is the parameter which would indicate the spanwise location where most of the energy interchange takes place since it is independent of the strip's span size.

Determination of the Spanwise Placement of an Active Control Surface

The determination of the best spanwise placement of an active control surface for flutter suppression requires the following steps to be made:

1. Determine the flutter dynamic pressure Q_F of the system.
2. Increase Q_F (so as to lie within the unstable region) and obtain the eigenvector $\{q_o\}$ of the unstable mode. The amount by which Q_F is increased is immaterial since only energy ratios are used herein. In the examples treated in this work, Q_F is increased so as to lie deep inside the unstable region.
3. Compute the matrices $[A]$ and $[A]^r$ for all the ℓ strips, at the reduced frequency appropriate for the unstable mode.
4. Since the system is unstable, W_A should assume a negative value (the system is doing a negative work on its surroundings per cycle of oscillation) when using equation (18).
5. Use equations (22) and (23) to compute the energy ratios $\bar{W}_A^r$ and the specific energy ratios $\bar{\bar{W}}_A^r$. Notice that negative values of $\bar{W}_A^r$ and $\bar{\bar{W}}_A^r$ indicate that the rth strip is absorbing energy from its surroundings (and thus contributing towards instability).
6. Determine the location of the strip $r = r_o$ where $\bar{\bar{W}}_A^r$ assumes the largest negative value.
7. The strip $r = r_o$ absorbs most energy per unit span and therefore would present the location where an active control surface would be most effective in suppressing flutter.

The above determination of the most effective placement of an active control surface for flutter suppression, as the location where maximum energy per unit span is fed into the system, is a natural consequence of the aerodynamic energy approach. It is shown in Nissim (1971; 1977) that a strip that absorbs energy from its surroundings can be made, by means of a suitable control law, to essentially stop absorbing energy and even made to be dissipative. On this basis, an active control surface placed at the location of maximum energy input will neutralize the maximum

energy input and may even turn to dissipate energy. This will clearly lead to maximum effectiveness regarding flutter suppression.

In cases where more than one critical flutter mode exists, the above procedure can be repeated for each flutter mode, and the two locations for the control surfaces can be determined. If a compromised single location for the control surface cannot be found, then two active control surfaces should be seriously considered.

It should be noted that

$$W_A = \sum_{r=1}^{\ell} W_A^r \tag{24}$$

Also, since W_A is negative by virtue of equations (2) and (3) above, the use of equations (22) and (24) yields

$$\sum_{r=1}^{\ell} \bar{W}_A^r = -1 \tag{25}$$

Note also that the integral over the spans of the specific energy ratios should be equal to -1. This follows from equation (23), whereby

$$\bar{W}_A^r = s_r \bar{\bar{W}}_A^r$$

and following equation (25)

$$\sum_{r=1}^{\ell} \bar{W}_A^r = \sum_{r=1}^{\ell} s_r \bar{\bar{W}}_A^r = -1 \tag{26}$$

Example Results

Three numerical examples are presented with the object of testing the method described above. These examples relate to the mathematical model of the drone for aerodynamic and structural testing—advanced research wing 2 (DAST–ARW2) aircraft used by NASA (Adams and Tiffany, 1985) to test active control concepts for flutter suppression, and they also relate to the mathematical model of the oblique wing aircraft developed by NASA. Figures 1, 2, and 3 show the geometrical descriptions of these models together with the aerodynamic panelling necessary for the computation of the aerodynamic coefficients using the doublet lattice method. Figures 1 and 3 also show the strip number allocations. In the following, the results obtained are presented and discussed for each of these two mathematical models.

Results for the DAST–ARW2 Mathematical Model

The DAST–ARW2 mathematical model employs two rigid body modes and ten elastic modes. It yields a flutter dynamic pressure $Q_F = 490$ lb/ft^2 (at $M = 0.85$) and a flutter frequency $\omega_F = 117$ rad/sec. The unstable eigenvector was computed for $Q = 550$ lb/ft^2 and the matrices $[A]$ and $[A]^r$ were computed for all 24 strips at the reduced frequency $k = 0.132$ associated with the unstable mode.

Figure 4 shows a plot of the specific energy ratios $\bar{\bar{W}}_A^r$ for the 17 strips along the wing. The first four strips (not shown in fig. 4) do not exchange any energy since they are on the vertical tail, and the flutter mode involves symmetrical mode shapes only. Strips 5 through 21 lie on the wing with strip 5 closest to the root and strip 21 closest

to the tip of the wing. It can be seen that the specific energy ratio is negative for all the wing strips, except for the root strip where $\bar{\bar{W}}_A^5$ is very small and positive. This indicates that all the wing strips (except for the root strip) absorb energy from the surroundings, and therefore, all the wing strips contribute to the instability of the system. The largest numerical value of $\bar{\bar{W}}_A^r$ relates to strip 18, which is the fourth strip inboard of the tip of the wing (coinciding with the inboard part of the aileron). Following the method presented herein, this is the best location for the aileron for purposes of flutter suppression. For a long aileron (as in the present case), its spanwise placement should be such that the aileron midspan point coincides with the midspan of strip 18 (that is, centered around the 80-percent span location). The remaining three strips (also not shown in fig. 4) lie on the horizontal tail, and they dissipate a negligible amount of energy. Note that the integration of $\bar{\bar{W}}_A^r$ over the span of the wing and the span of the horizontal tail should be equal to -1. Note also that the area of $\bar{\bar{W}}_A^r$ along the rth strip is equal to the energy ratio $\bar{W}_A^r$. In conclusion, it can be stated that from the point of view of active flutter suppression, the aileron could be placed a little more inboard of its present location. Such an inboard shift can also contribute to an increase in the effectiveness of the activated control surface in gust and load alleviation (Nissim and others, 1976).

Results for the Oblique Wing Mathematical Model

Figures 2 and 3 show the geometrical description of the oblique wing model with the right wing swept forward at an angle of 65° (Burken and others, 1986), together with the doublet lattice aerodynamic panelling and the strip number allocations. The model is asymmetric, and it involves five rigid body modes and fifteen elastic modes. A flutter computation at Mach 0.95 shows that a mild, 78 rad/sec, vertical tail flutter instability develops around Q_F = 780 lb/ft^2. Flutter reaches its peak instability at Q = 1600 lb/ft^2 and it remains unstable thereafter with the instability getting milder as Q increases. This instability can be turned into a neutrally stable oscillation by introducing a 2.5 percent structural damping. However, even in this latter case, one would expect a large dynamic response of this specific mode, with serious effects on the fatigue life of the aircraft, thus warranting the consideration of active controls for either stabilization or gust alleviation purposes. The specific energy ratio distribution, as presented in this work, was computed for Q = 1600 lb/ft^2 and the results are presented in figure 5.

It should be noted that strips 1 through 4 lie on the vertical tail, with strip 1 near the root and strip 4 near the tip. Strip 5 represents the vertical projection of the fuselage and is not shown in figure 5 ($\bar{\bar{W}}_A$ in strip 5 equals 0.011). Strips 6 through 22 lie on the wing, with strip 6 at the left tip of the wing and strip 22 at the right tip of the wing. Strips 23 through 26 lie on the left horizontal tail, with strip 23 at the left tip and strip 26 at the root of the left horizontal tail. Strips 27 and 28 represent the horizontal projection of the fuselage (from left to right). Finally, strips 29 through 32 lie on the right horizontal tail, with strip 29 close to the root and strip 32 at the tip of the right horizontal tail.

Figure 5 shows that most of the energy input into the system takes place through the vertical tail and some through the inboard strips of the horizontal tail and the horizontal projection of the fuselage. It should also be noted that the wing, the vertical fuselage, and the outboard portions of the horizontal tail play a stabilizing role (with most of the wing strips dissipating energy). It is this dissipation of energy that leads to the mild flutter instability exhibited in this case. Figure 5 clearly shows that for the suppression of this flutter mode, the active control surface should be placed around the center of strip 3 of the vertical tail (that is, around the 60-percent span location). For a long control surface, centering the activated control around the 50-percent span location would be more appropriate considering the distribution of the specific aerodynamic energy ratios shown in figure 5(a).

Results for a Modified Oblique Wing Mathematical Model

The oblique wing model is unique from the point of view of asymmetry. The best placement of an activated control surface along its span could present an interesting challenge. Therefore, it was decided to modify the oblique wing

mathematical model so as to force the wing to flutter. This was done by considerably lowering one of the torsional frequencies of the wing from 45 to 12 Hz. Therefore, the results to be described in the following *do not* relate to the actual wing but to a synthetically modified wing.

The above modified model of the oblique wing yields two flutter speeds: (1) around Q_F = 750 lb/ft^2 and ω_F = 79 rad/sec, and (2) around Q_F = 1050 lb/ft^2 and ω_F = 70 rad/sec. The first flutter mode is found to be essentially the same as the one already described in the previous section of this work (although its mildness is somewhat reduced), and, therefore, the results pertaining to this mode will not be repeated. In the following, the results relating to the second mode will be described using an eigenvector obtained at Q =1300 lb/ft^2.

The specific energy ratio distribution over the different strips of the aircraft is shown in figure 6. It can be seen that most of the energy input to the system takes place through the wing strips, with some additional energy input through the left horizontal tail and still smaller contributions from the inboard strips of the vertical tail. Some energy is dissipated mainly at the outboard portions of the vertical tail, the right horizontal tail, and at some of the wing's strips around its central portion and the extreme right wingtip. Since the wing is essentially responsible for most of the energy input to the system, it is interesting to note the effect of the asymmetry of the aircraft on the energy input to the wing. Figure 6(b) shows that the strips located around the left tip of the wing are responsible for most of the energy input, with the left tip strip (strip 6) showing the largest value for the specific energy ratio. Hence, for the suppression of this flutter mode, the activated control surface should be placed as close to the left wingtip as is structurally possible. Strips 9 and 10 can also form a reasonable alternative to the extreme tip placement of the activated control surface, that is, around the 65-percent span location of the left wing.

The results presented above regarding the responsibility of the left-most strips of the left wing to the absorption of energy which leads to flutter seem surprising and also puzzling. At this stage, it should be stated that the wing plane is located 50 in. above the horizontal tail plane. It should be expected that a strong wing-tail interference between the left horizontal tail and the tip portion of the left wing will take place. Therefore, it is possible that the flutter instability in this case is a result of this interference between the above two lifting surfaces.

CONCLUDING REMARKS

The method developed in this work enables the determination of the spanwise placement of activated control surfaces for purposes of flutter suppression without resorting to any specific control law. The examples used indicate a range of such locations, depending on the flutter mode. It is expected that flutter modes due to external stores will indicate still other spanwise placements when compared to those obtained in this work. Where more than one critical flutter speed exists requiring neighboring placements of active control surfaces, the placement of a single activated control surface at a compromise location can be examined. An example where such a compromise cannot be made is given in the modified oblique wing example, where activated controls need to be placed both along the vertical tail and the left wing outboard region.

Ames Research Center
Dryden Flight Research Facility
National Aeronautics and Space Administration
Edwards, California, May 10, 1988

REFERENCES

Adams, W.M., Jr., and S.H. Tiffany, "Development of a Flutter Suppression Control Law by Use of Linear Quadratic Gaussian and Constrained Optimization Design Techniques," 2nd International Symposium on Aeroelasticity and Structural Dynamics, Apr. 1985, West Germany.

Albano, E., and W.P. Rodden, "A Doublet-Lattice Method for Calculating Lift Distributions on Oscillating Surfaces in Subsonic Flows," *AIAA Journal*, vol. 7, no. 2, Feb. 1969, pp. 279–285.

Burken, John J., Gurbux S. Alag, and Glenn B. Gilyard, *Aeroelastic Control of Oblique-Wing Aircraft*, NASA TM-86808, 1986.

Mahesh, J.K., C.R. Stone, W.L. Garrard, and H.J. Dunn, "Control Law Synthesis for Flutter Suppression Using Linear Quadratic Gaussian Theory," *AIAA Journal of Guidance and Control*, vol. 4, no. 4, July–Aug. 1981, pp. 415–422.

Mori, A.S., and J.H. Wykes, "Techniques and Results of an Analytical Investigation Into Controlling the Structural Modes of Flexible Aircraft," AIAA Symposium on Structural Dynamics and Aeroelasticity, Boston, Aug.–Sept. 1965, pp. 419–433.

Mukhopadhyay, Vivek, Jerry R. Newsom, and Irving Abel, *A Method for Obtaining Reduced-Order Control Laws for High-Order Systems Using Optimization Techniques*, NASA TP-1876, 1981.

Newsom, Jerry R., *A Method for Obtaining Practical Flutter-Suppression Control Laws Using Results of Optimal Control Theory*, NASA TP-1471, 1979.

Nissim, E., *Flutter Suppression Using Active Controls Based on the Concept of Aerodynamic Energy*, NASA TN D-6199, 1971.

Nissim, E., *Recent Advances in Aerodynamic Energy Concept for Flutter Suppression and Gust Alleviation Using Active Controls*, NASA TN D-8519, 1977.

Nissim, E., and Irving Abel, *Development and Application of an Optimization Procedure for Flutter Suppression Using the Aerodynamic Energy Concept*, NASA TP-1137, 1978.

Nissim, E., A. Caspi, and I. Lottati, *Application of the Aerodynamic Energy Concept to Flutter Suppression and Gust Alleviation by Use of Active Controls*, NASA TN D-8212, 1976.

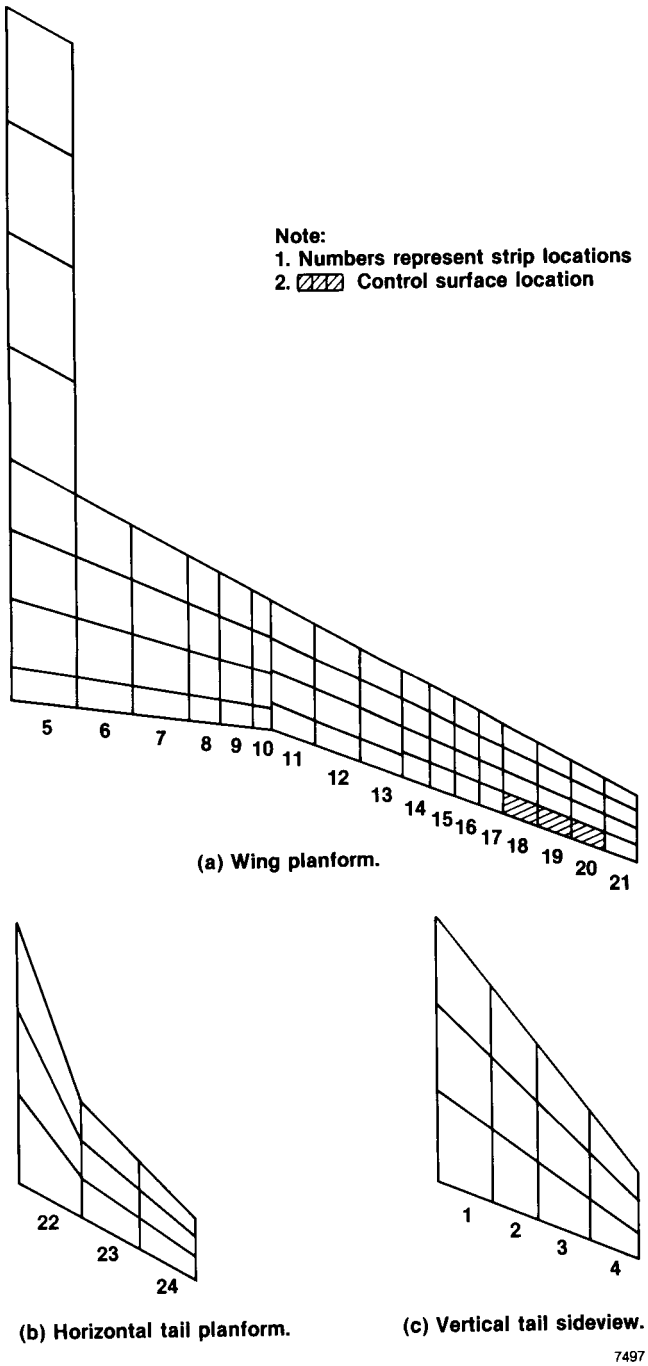

Figure 1. DAST–ARW2 model geometric layout, together with doublet lattice panelling and strip number allocations.

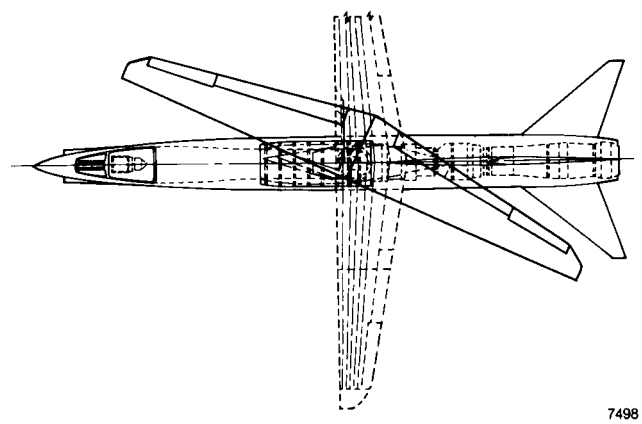

Figure 2. Oblique wing model—planform view with wing skewed 65°.

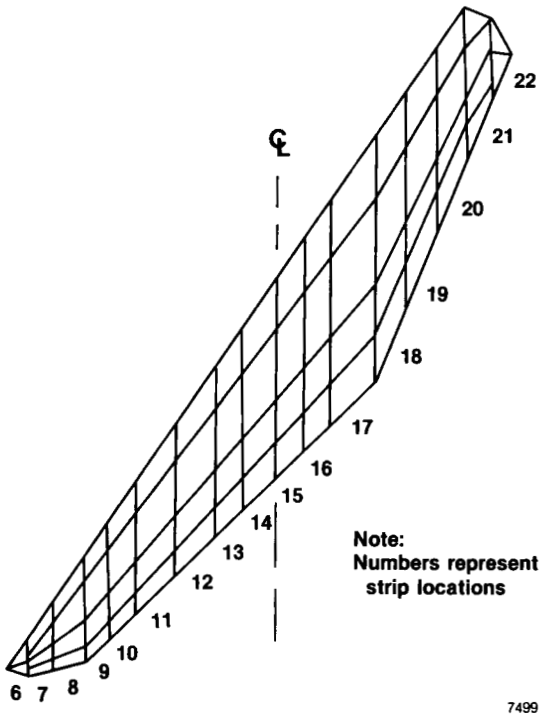

(a) Oblique wing planform skewed 65°.

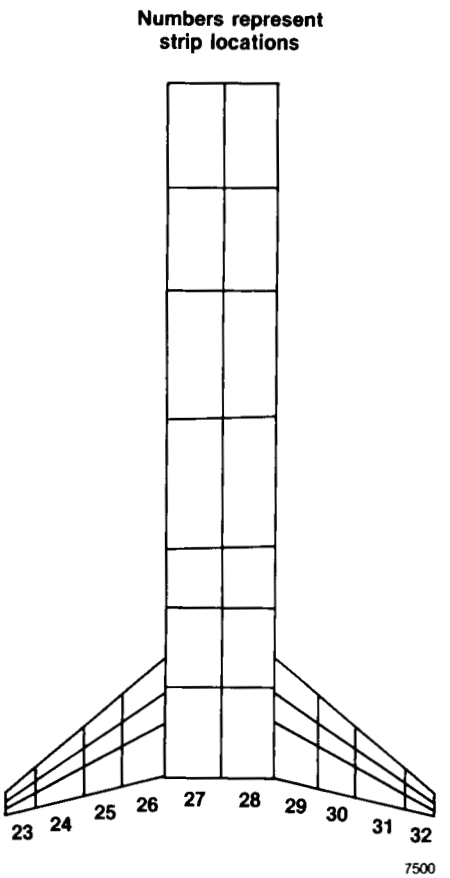

(b) Horizontal tail and horizontal projection of the fuselage planform.

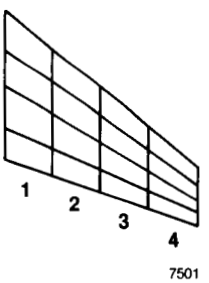

(c) Vertical tail sideview.

Figure 3. Oblique wing model—geometric layout together with doublet lattice panelling and strip numbers.

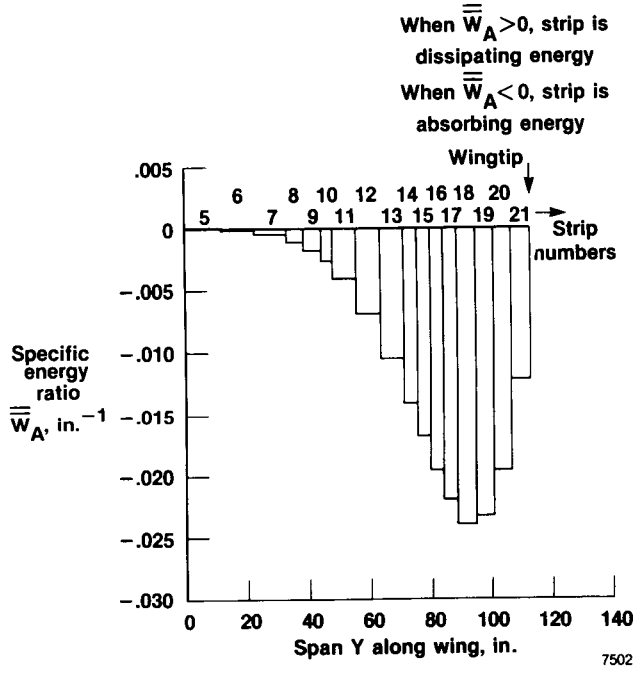

Figure 4. DAST–ARW2 model, variation of specific energy ratio $\bar{\bar{W}}_A$ with strip locations along the wing.

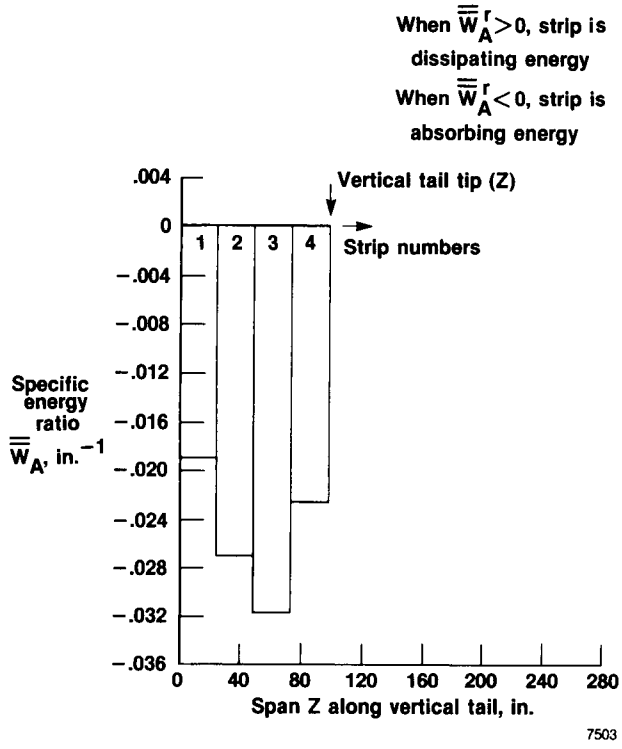

(a) Vertical tail.

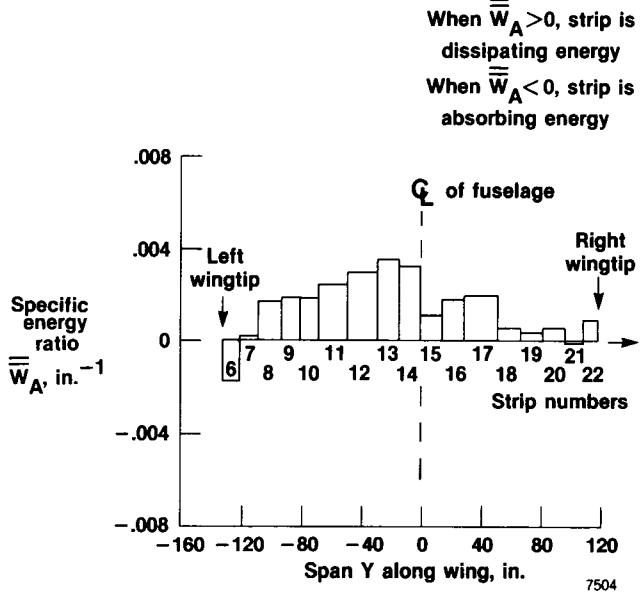

(b) Wing.

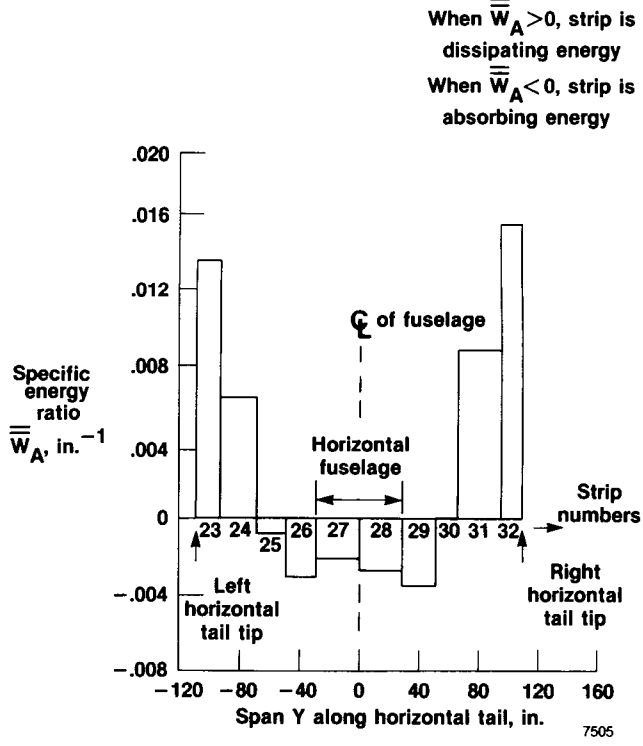

(c) Horizontal tail and horizontal fuselage.

Figure 5. Oblique wing model—variation of specific energy ratio $\bar{\bar{W}}_A$ with strip locations.

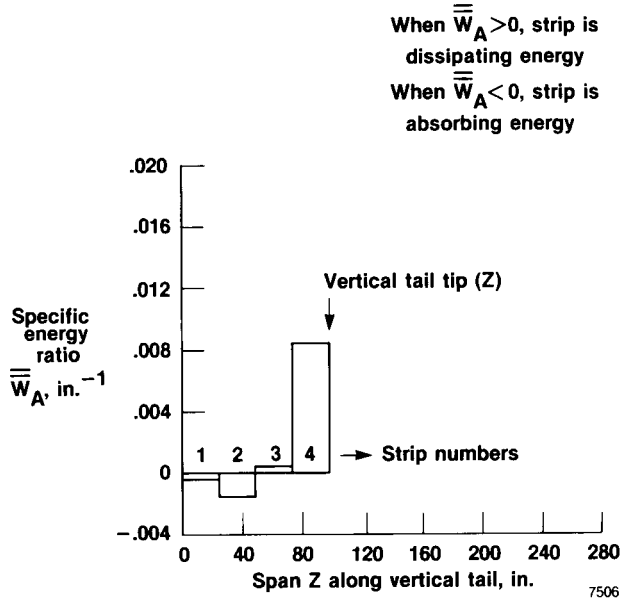

(a) Vertical tail.

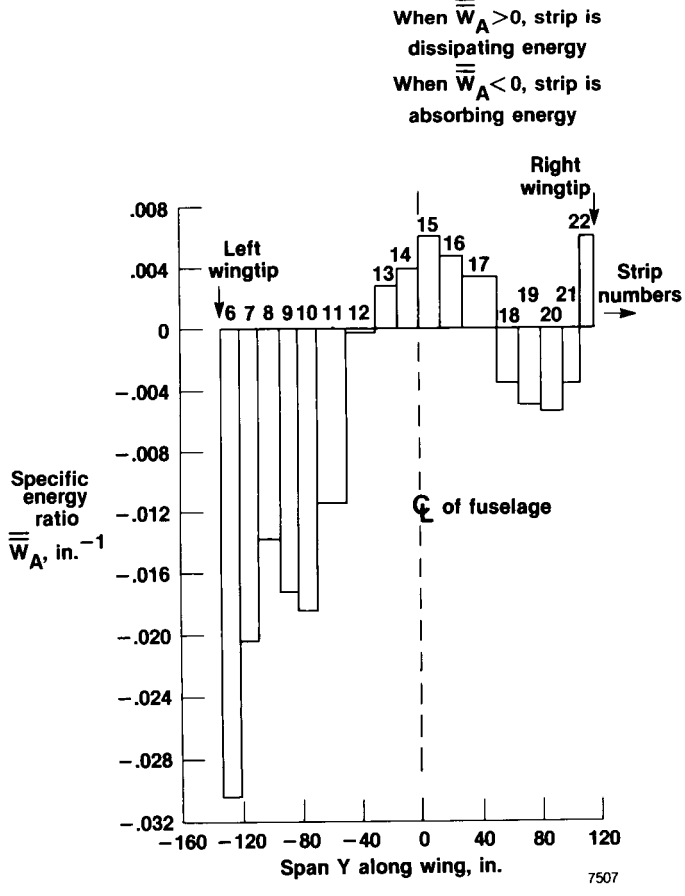

(b) Wing.

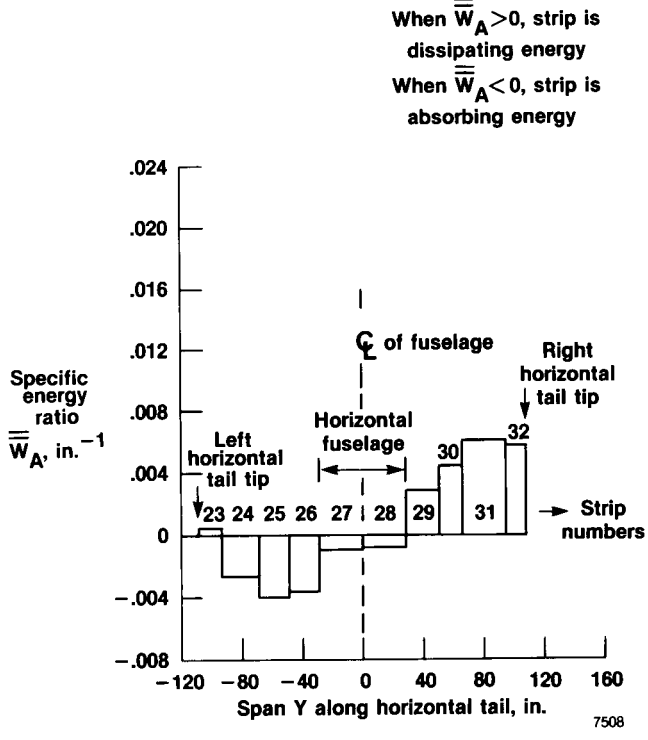

(c) Horizontal tail and horizontal fuselage.

Figure 6. Modified oblique wing model—variation of specific energy ratio $\bar{\bar{W}}_A$ with strip locations.

NASA
National Aeronautics and Space Administration

Report Documentation Page

1. Report No.	2. Government Accession No.	3. Recipient's Catalog No.
NASA TP-2873		

4. Title and Subtitle

Control Surface Spanwise Placement in Active Flutter Suppression Systems

5. Report Date

November 1988

6. Performing Organization Code

7. Author(s)

E. Nissim and John J. Burken

8. Performing Organization Report No.

H-1492

10. Work Unit No.

RTOP 505-66-71

9. Performing Organization Name and Address

NASA Ames Research Center
Dryden Flight Research Facility
P.O. Box 273, Edwards, CA 93523-5000

11. Contract or Grant No.

13. Type of Report and Period Covered

Technical Paper

12. Sponsoring Agency Name and Address

National Aeronautics and Space Administration
Washington, DC 20546

14. Sponsoring Agency Code

15. Supplementary Notes

This research was undertaken while Eli Nissim held a National Research Council – NASA (Ames Research Center, Dryden Flight Research Facility) Research Associateship. The author was on leave from Technion – Israel Institute of Technology.

16. Abstract

A method is developed that determines the placement of an active control surface for maximum effectiveness in suppressing flutter. No specific control law is required by this method which is based on the aerodynamic energy concept. It is argued that the spanwise placement of the active controls should coincide with the locations where maximum energy per unit span is fed into the system. The method enables one to determine the distribution, over the different surfaces of the aircraft, of the energy input into the system as a result of the unstable fluttering mode. The method is illustrated using three numerical examples.

17. Key Words (Suggested by Author(s))

Active controls
Aeroservoelasticity
Flutter suppression

18. Distribution Statement

Unclassified — Unlimited

Subject category 39

19. Security Classif. (of this report)	20. Security Classif. (of this page)	21. No. of pages	22. Price
Unclassified	Unclassified	20	A02

NASA FORM 1626 OCT 86

*For sale by the National Technical Information Service, Springfield, VA 22161-2171.

NASA-Langley, 1988